Electronic Supplementary Material (ESI) for Materials Horizons.

Acid Dyeing for Green Solvent Processing of Solvent Resistant Semiconducting Organic Thin Films

SUPPORTING INFORMATION

Cayley R. Harding,[a] Jonathan Cann,[a] Audrey Laventure,[a] Mozhgan Sadeghianlemraski,[b] Marwa Abd-Ellah,[a,b] Keerthan R. Rao,[d] Benjamin Sidney Gelfand,[a] Hany Aziz,[b] Loren Kaake,[c] Chad Risko,[d] Gregory C. Welch[a]*

[a] Department of Chemistry, University of Calgary, 2500 University Drive N.W., Calgary, Alberta, Canada, T2N 1N4
[b] Department of Electrical and Computer Engineering, University of Waterloo, Waterloo, Ontario, Canada, N2L 3G1
[c] Department of Chemistry, Simon Fraser University, Vancouver, British Columbia, Canada, V5A 1S6
[d] Department of Chemistry & Center for Applied Energy Research, University of Kentucky, Lexington, Kentucky, USA, 40506

*E-mail : gregory.welch@ucalgary.ca

Table of Contents

1. Materials and Methods

UV-Visible Spectroscopy (UV-Vis): Measurements were recorded using an Agilent Technologies Cary 60 UV-Vis spectrometer at room temperature. All solution UV-Vis experiments were run using 10 mm quartz cuvettes. Films were spin-coated onto PET substrates.

Atomic Force Microscopy (AFM): AFM measurements were performed by using a TT2- AFM (AFM Workshop) in tapping mode and WSxM software with a tip at a resonance frequency of 300 kHz, a force constant of 40 N/m and a reflective back side aluminum coating (Tap300Al-G, BudgetSensors).

Optical Light Microscopy: Images were taken using a BX53 Olympus Scope.

Single Crystal X-ray Crystallography: Single crystals of $C_{34}H_{29}N_3O_4$ **PDIN-H** were grown by vapour diffusion at room temperature of methanol into a solution of **PDIN-H** in dioxane. A suitable crystal was selected and mounted on a glass loop using Paratone oil. Diffraction experiments were performed on a Bruker Smart diffractometer equipped with an Incoatec Microfocus (Cu Kα, λ = 1.54178 Å) and an APEX II CCD detector. The crystal was kept at 173 K during data collection. Diffractions spots were integrated and scaled with SAINT[1] and the space group was determined with XPREP[2]. Using Olex2,[3] the structure was solved with the ShelXT[4] structure solution program using Intrinsic Phasing and refined with the ShelXL[5] refinement package using Least Squares minimisation.

Table S1. Crystal data and structure refinement for PDIN-H

Empirical formula	$C_{34}H_{29}N_3O_4$
Formula weight	543.60
Temperature/K	173
Crystal system	monoclinic
Space group	$P2_1/c$
a/Å	18.2166(7)
b/Å	18.5973(10)
c/Å	7.8095(2)
α/°	90
β/°	97.881(2)
γ/°	90
Volume/Å^3	2620.71(19)
Z	4
ρ_{calc}g/cm^3	1.378
μ/mm^{-1}	0.734
F(000)	1144.0
Crystal size/mm^3	0.358 × 0.11 × 0.086
Radiation	CuKα (λ = 1.54178)
2θ range for data collection/°	4.898 to 130.452
Index ranges	$-21 \leq h \leq 21$, $-21 \leq k \leq 21$, $-9 \leq l \leq 9$
Reflections collected	22039
Independent reflections	4467 [R_{int} = 0.0349, R_{sigma} = 0.0216]
Data/restraints/parameters	4467/0/378
Goodness-of-fit on F^2	1.026
Final R indexes [I>=2σ (I)]	R_1 = 0.0581, wR_2 = 0.1587
Final R indexes [all data]	R_1 = 0.0639, wR_2 = 0.1639
Largest diff. peak/hole / e Å^{-3}	0.57/-0.29

Computational methods: All density functional theory (DFT) and time-dependent DFT (TDDFT) calculations were carried in the Gaussian16 (Revision A.03) software suite.[6] The M06 functional[7] was employed with the 6-31G(d,p) Pople basis set.[8-10] Normal mode analyses were carried out for optimized geometries to ensure that no negative frequencies were present. The SMD implicit solvation model[11] was used to compute the fixed concentration free energies of solvation in 1-propanol. The combination of computed free energies and gas phase energies were employed to determine the pK_a. TDDFT calculations provided the excited-state transitions up to 10 states. Absorption spectra were simulated through convolution of the vertical transition energies and oscillator strengths with Gaussian functions characterized by a full width at half-maximum (fwhm) of 0.33 eV. Pictorial representations of the molecular orbitals were visualized using GaussView 5.0.9.[12]

Determination of pKa. To calculate the pK_a of PDINH in solution, we followed the methods described by Ho and co-workers and others, using 1-propanol as the solvent.[13-18] The gas phase free energy of the proton ($\mathbf{G^o_g(H^+)}$) was taken to be −26.3424 kJ/mol, [19] while the proton solvation free energy ($\Delta\mathbf{G_s^*(H^+)} = -1104.7642$ kJ/mol in 1-propanol) was determined as described by Lee *et al.* [20] and using semi-empirical data.[21-22] Along with the electronic and thermal free energies of the species,[13] the following equations were employed to calculate the pK_a,

$$\Delta\mathbf{G^*_s = G_{soln}(R_l) - G_{gas}(R_g)}$$

The solution phase and the gas phase geometries are labelled as R_l and R_g respectively.

$$\mathbf{\Delta G^*_{soln} = \Delta G^*_{gas} + \Delta G^*_s(H^+) + \Delta G^*_s(A^-) - \Delta G^*_s(HA)}$$

$$\mathbf{pK_a(HA) = \frac{\Delta G^*_{soln}}{RT\ ln(10)}}$$

The pKa of a single PDINH molecule optimized in 1-propanol was determined to be 19.7.

Hydrogen bond strength in the crystal. The strength of the hydrogen bond of NH••O=C was determined by computing the electronic and thermal free energies of the dimerized PDINH and single molecule PDINH in the gas phase. The strength of the hydrogen bond was determined using the supramolecular approach,

$$\Delta\mathbf{E_{H\text{-}bond} = E_{stacked\_PDINH} - (2\times E_{PDINH})}$$

where, $\Delta\mathbf{E_{H\text{-}bond}}$ is the strength of the NH••O=C hydrogen bond, $\mathbf{E_{stacked\_PDINH}}$ is the electronic and thermal free energy of the stacked-PDINH and $\mathbf{E_{PDINH}}$ is the electronic and thermal free energy of a single PDINH molecule. The binding energy due to the hydrogen bond was determined to be −10.14 kcal/mol.

General Coating Parameters: Spin-coated films were coated at room temperature at a speed of 1000 rpm for 60 s. Slot-die coated films were coated using a compact sheet coater from FOM Technologies equipped with a 13 mm wide slot-die head using a solution dispense rate ranging from 90 to 140 μL/min depending on solvent and a substrate motion speed of 30 cm/min.

Slot-die coating was performed with a FOM compact sheet coater under ambient conditions (A). For coatings the slot-die head was cleaned and assembled with 13 mm shim (B and C), then attached to the sheet coater (D). Approximately 2 mL of solution was loaded into a 5 mL Luer-Lok syringe and needle. The syringe was held upright and air expelled. The needle was removed, and Luer-Lok syringe was connected to P-628 Luer female adapter then attached to 1521 FEP tubing (inner diameter: 1.75 mm) via a P-330X flangeless male nut and P-300X flangeless ferrule (E and F). Solution was pushed ¾ of way through tubing. The loaded syringe and tubing were inserted into syringe holder (G) on pump and the other end of tubing (with a P-330X flangeless male nut and P-300X flangeless ferrule) was attached to the slot die head for the final setup (H). Substrate was loaded onto flatbed (PET – gloss waterproof inkjet film provided from Printing Supplies Direct); dust was removed via a Teknek contact cleaning hand roller. Slot-die head was moved to starting point, lowered (until shim is around 1 cm from substrate) and pump started (2 mL/min until solution was in the slot-die head). Printing conditions of pump dispense rate, length of print, and substrate motion speed were selected, pump dispense rate changing with various solvents, length of print changing according to length required, and substrate speed remaining constant at 30 cm/min. Once optimum dispense rate was selected (known from previous testing), the pump was run until solution followed shim out of the slot-die head, pump was stopped, and meniscus was formed with substrate (by lowering slot-die head). Amount dispensed was zeroed on machine, pump was turned on followed immediately by the movement of the substrate. After coating the pump would be stopped about 1s before the substrate finished moving to prevent significant pooling of the ink. The slot-die head was raised to break meniscus and moved accordingly to repeat process on another part of substrate if required. All substrates were allowed at least 30 minutes to dry on flatbed before removal, cut to 1.5 cm x 1.5 cm samples after an hour, and allowed to dry in petri dishes overnight in drawer before being subject to analysis. For slot-die coated solvent resistant tests neat solvents were loaded into a cleaned syringe and coated directly on top of previously coated films.

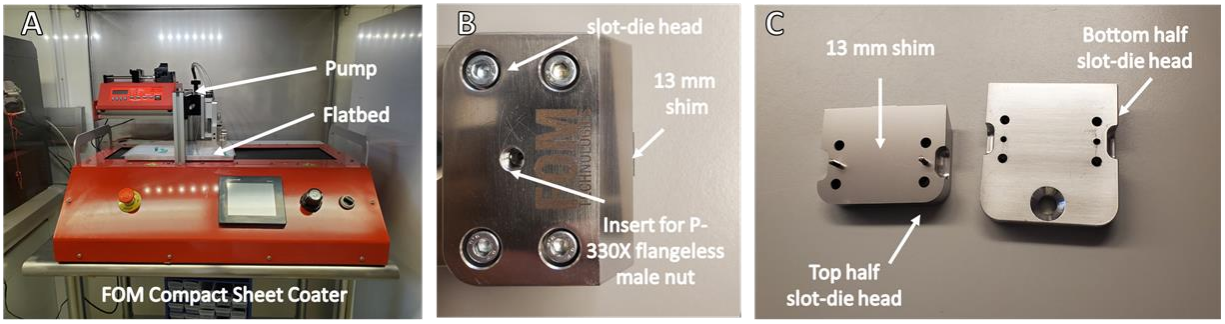

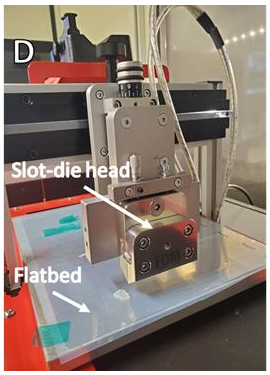
D
Slot-die head
Flatbed

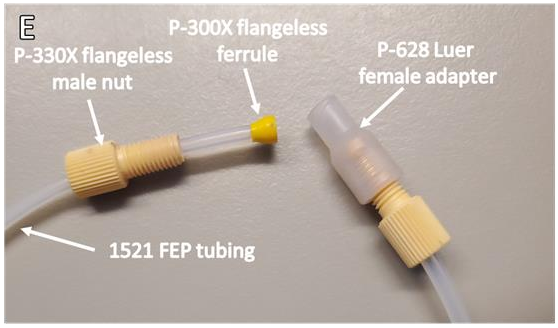
E
P-330X flangeless male nut
P-300X flangeless ferrule
P-628 Luer female adapter
1521 FEP tubing


F
5 mL Luer-Lok syringe

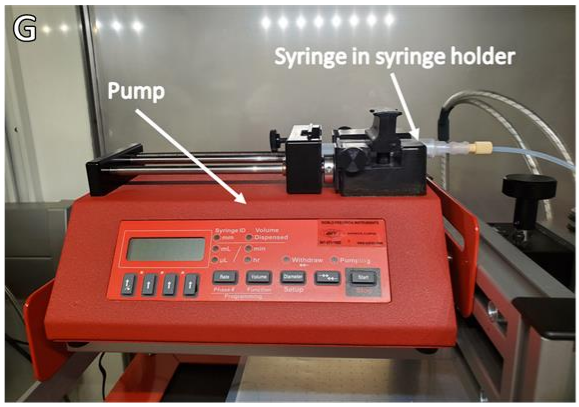
G
Pump
Syringe in syringe holder

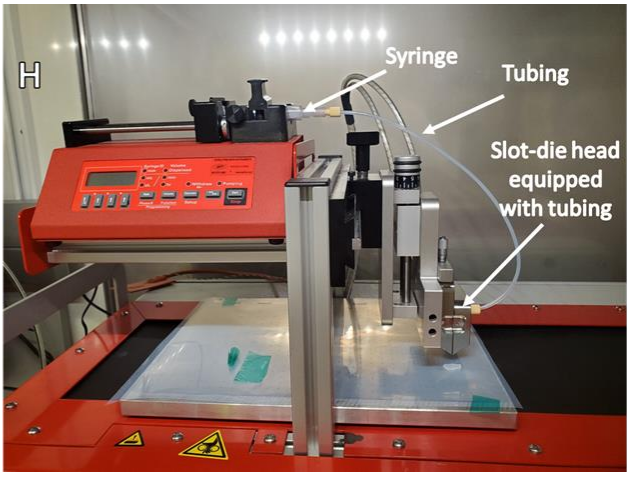
H
Syringe
Tubing
Slot-die head equipped with tubing

Organic Photovoltaics:

***Material Preparation*:** For ZnO sol–gel preparation, 197 mg zinc acetate was dissolved in a 6 mL ethanol plus 54 μL ethanolamine while mixing at 45 °C and 650 rpm for 50 min. To prepare the PDIN-Na solution, 10 mg/ml of sodium hydroxide (NaOH) was dissolved in 1-propanol through stirring at 400 rpm for 30 min. Then, 0.162 mL of this solution was added to a mixture of 1-propanol (2 mL) and PDIN-H (10 mg) followed by stirring at 400 rpm for 30 min. The solution was filtered through a 0.22 μm polypropylene filter prior to film formation. For the active layer, a 45 mg/ml solution of poly(3-hexylthiophene) (P3HT): [6,6]-Phenyl C_{61} butyric acid methyl ester ($PC_{60}BM$), (1:1), in dichlorobenzene was prepared by stirring at 100 ° C and 650 rpm overnight inside the glovebox. The solution was filtered through a 0.22 μm PTFE filter prior to film formation.

***Device Fabrication*:** For OPV device fabrication, ITO-patterned glass substrates (Kintec) with a thickness of 80 nm and a sheet resistance of 15 Ω sq^{-1} were used. The substrates were first cleaned via sequential ultrasonic cleaning using Micro 90, deionized water, acetone and isopropanol solutions, following 5 min of O_2 plasma treatment. For coating the electron transport layers (ETL), ZnO was spin-coated at 1000 rpm for 60 s and annealed at 150 °C for 30 min, and PDIN-Na solution was spin coated at 4000 rpm for 60 s followed by annealing at 120 °C for 10 min. The P3HT:$PC_{60}BM$ solution was spin coated at 1000 rpm for 80 s and thermally annealed at 150°C for 30 min inside the glovebox, resulting in a 150 nm thick bulk heterojunction (BHJ) active layer. The ITO-patterned substrate consisted of 12 OPVs with a surface area of 0.04 cm^2 of each. To compare the different ETLs more accurately, each substrate was first cut into four equal pieces, and the corresponding solution processes of each ETL were done on one piece. Then, the four pieces were taped together and transferred into an Angstrom Engineering EvoVac thermal evaporation chamber with a base pressure of 5×10^{-6} Torr for deposition of 5 nm of MoO_3 (American Elements), and 100 nm of aluminum anode (Angstrom Engineering).

Material and Device Characterization: Measurements of current density–voltage characteristics were carried out by a Keithley 2400 source, under 1-sun AM1.5G illumination from an ABET Sun 3000 Class AAA solar simulator. The external quantum efficiency (EQE) measurements were performed using the PV measurement (QEX10) system. The cells are illuminated under a monochromatic light, achieved though filtering a xenon arc lamp source, coupled with a germanium photodiode, by a dual-grating monochromator.

Table S2. OPV Device parameters (champion)

ETL	J_{sc} (mA/cm^2)	V_{oc} (mV)	FF [%]	PCE [%]
ZnO	7.0	663	60	2.8
ZnO/PDIN-H	6.9	652	59	2.7
PDIN-H	6.8	646	53	2.3
none	8.3	577	41	1.9

Device: Glass/ITO/ETL/P3HT:$PC_{60}BM$/MoOx/Al

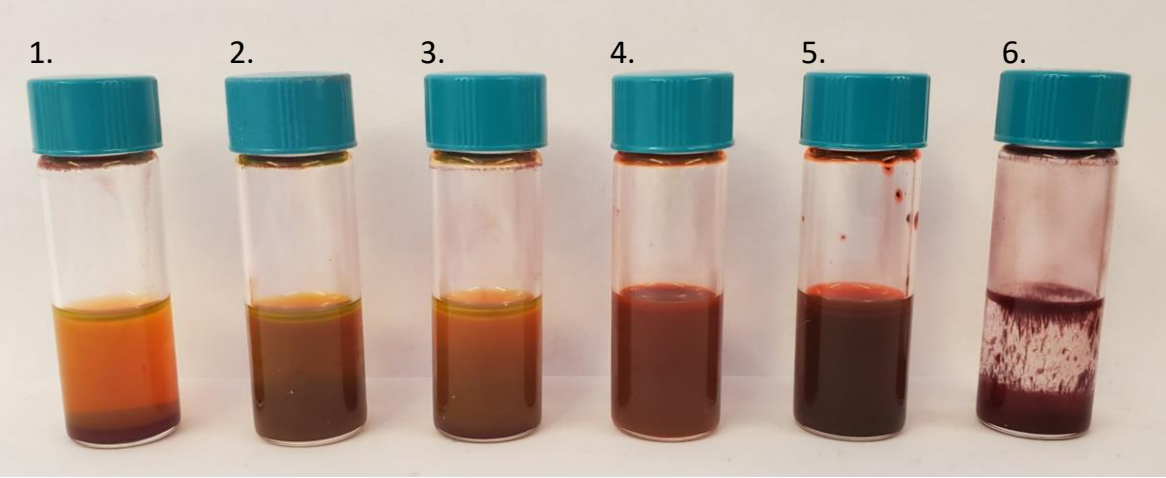

Figure S1. Mixtures of 5 mg/mL PDIN-H in various solvents to demonstrate the low solubility of the PDI-NH compound in: 1. 1-propanol, 2. Dichloromethane, 3. *o*-xylene, 4. Chloroform, 5. Dimethyl formamide, 6. Hexanes.

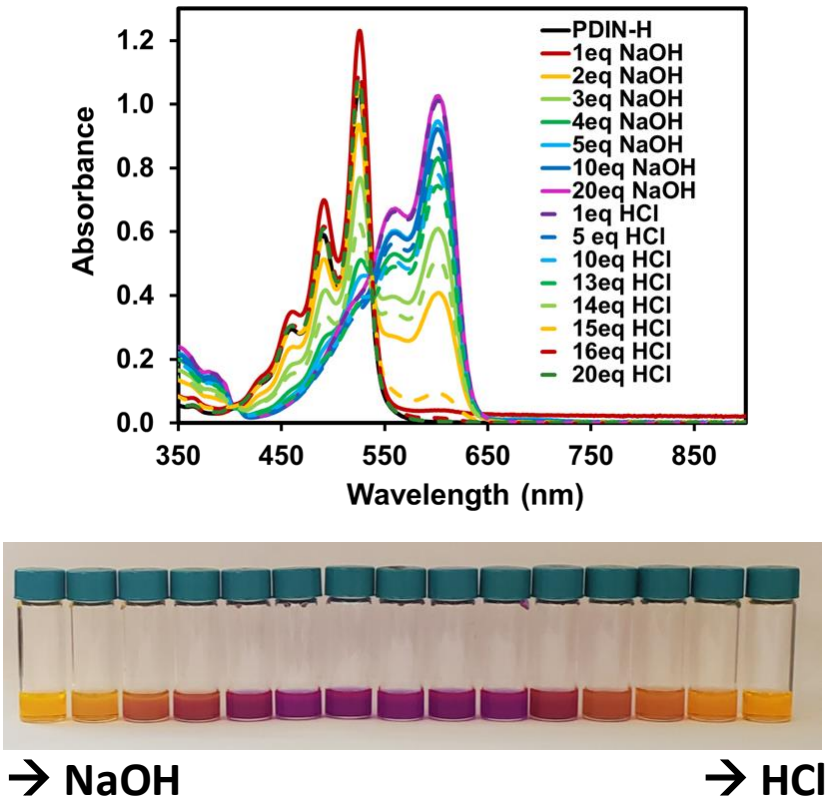

Figure S2. UV-vis spectra for 0.05 mg/mL PDIN-H solutions in n-propanol with molar equivalents of NaOH and HCl added sequentially. NaOH added PDIN-H followed by adding HCl to the formed PDIN- anion. This experiment shows that the deprotonation of PDIN-H is fully reversible. Pictures of the solutions shown.

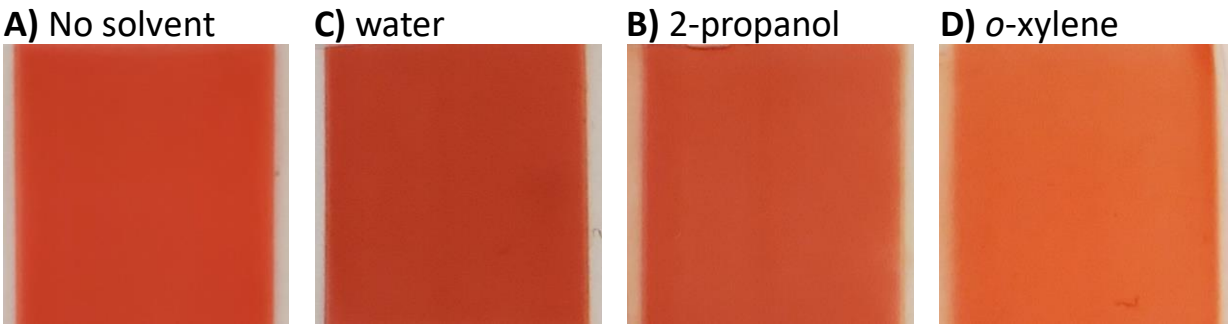

Figure S3. Photographs (1.5 cm x 1.5 cm) for PDIN-H slot-die coated films dipped in various solvents for 10 s and allowed to air dry. Films were formed by slot-die coating a solution of PDIN-H in 1-propanol (10 mg/mL) with 1 molar equivalent of NaOH added.

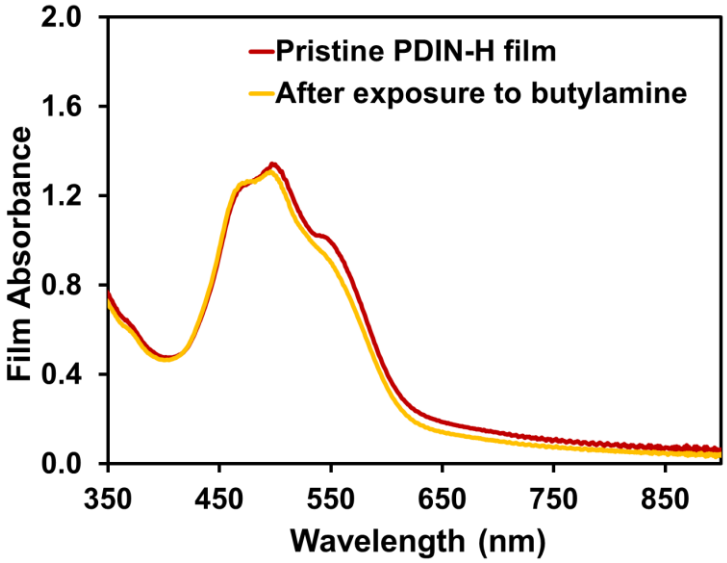

Figure S4. UV-vis spectra of slot-die coated PDIN-H from 1-propanol (10 mg/mL) with 1 molar equivalent of NaOH before and after exposure to butylamine vapor for 1 minute (1 mL of butylamine was deposited at the bottom of a closed container and the film was placed on a watch glass in this container – the film turned purple, after 1 minute the container was opened to remove all butylamine – the film turned red).

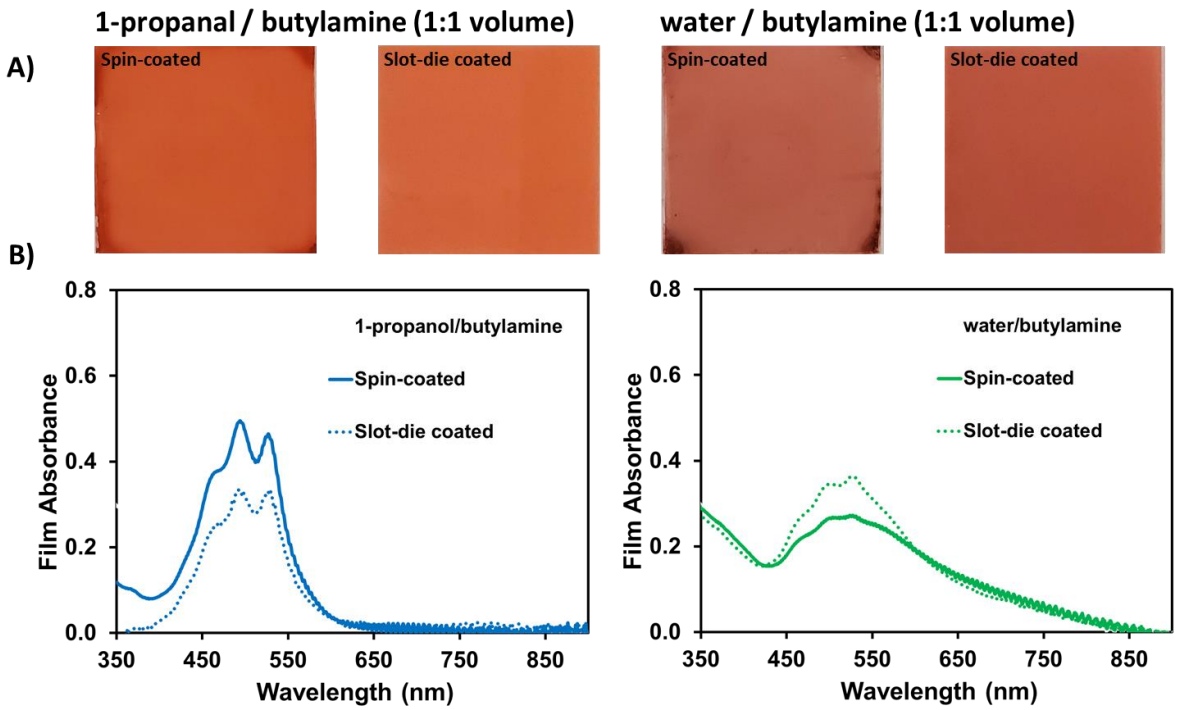

Figure S5. A) Top left to right, photographs (1.5 cm x 1.5 cm) – spin-coated PDIN-H in 1-propanol (10 mg/mL) with added volume equivalents of butylamine on PET. Slot-die coated PDIN-H in 1-propanol (10 mg/mL) with added volume equivalents of butylamine on PET. Spin-coated PDIN-H in water (10 mg/mL) with added volume equivalents of butylamine on PET. Slot-die coated PDIN-H in water (10 mg/mL) with added volume equivalents of butylamine on PET. B) UV-vis absorptance spectra of the above mentioned films.

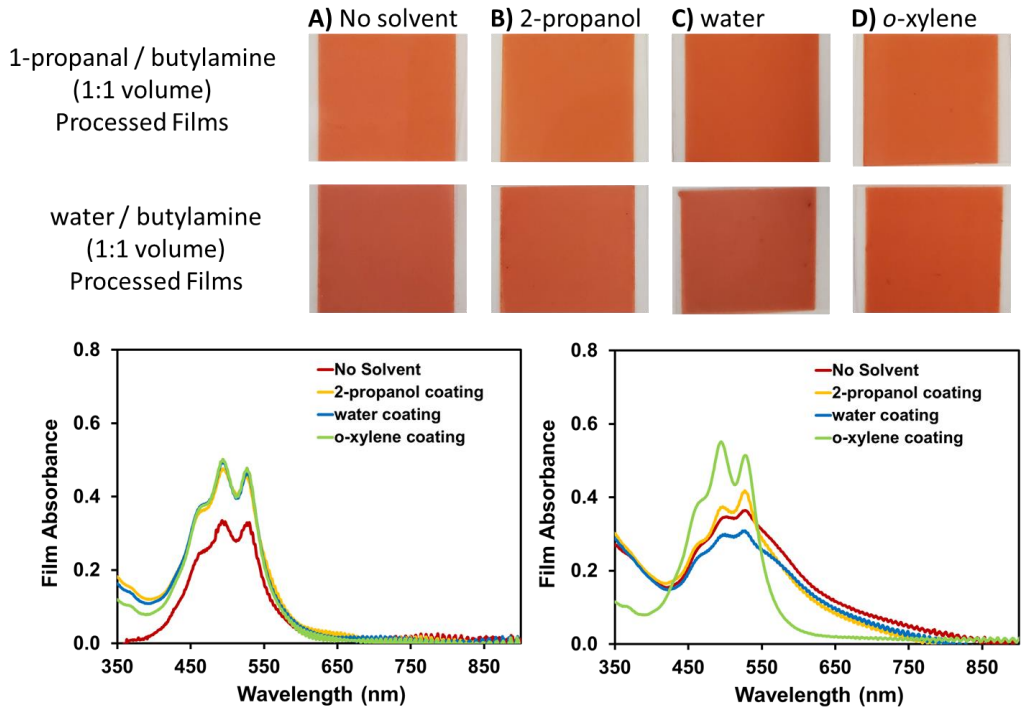

Figure S6. Photographs (1.5 cm x 15.cm, top), and UV-vis spectra (bottom) for PDIN-H films A) as-cast with no solvent coated on top and with B) 2-propanol, C) water, or D) *o*-xylene slot-die coated on top and left to dry. PDIN-H films formed via slot-die coating 10 mg/mL PDIN-H solutions in 1-propanol or water with 1 volumetric equivalent of butylamine added. Left UV-vis spectra show 1-propanol/butylamine films and right show water/butylamine films.

Appendix S1

Safety comment and hazards information

All slot-die coating was done under fume hood to prevent possible irritations, volatile solvents (alcohols and amines) were kept away from heat or open flame. Otherwise, no expected or unusually high safety hazards were encountered.

1-octanol

https://pubchem.ncbi.nlm.nih.gov/compound/1-Octanol accessed March 05, 2020

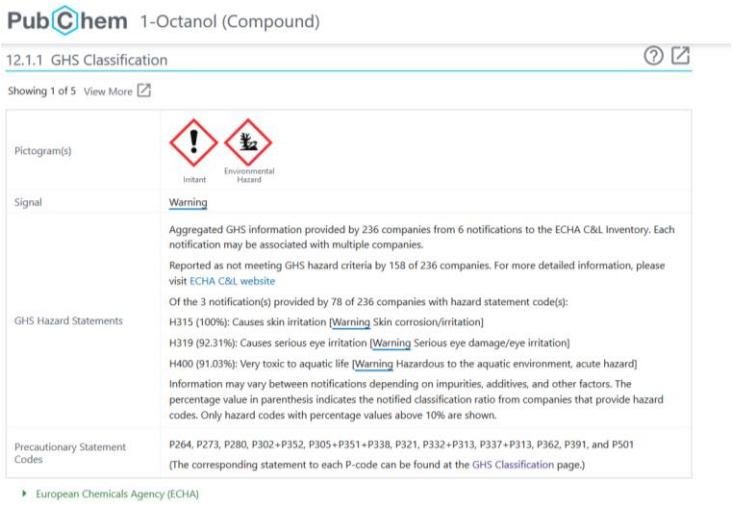

1-nonanol

https://pubchem.ncbi.nlm.nih.gov/compound/8914 accessed March 05, 2020

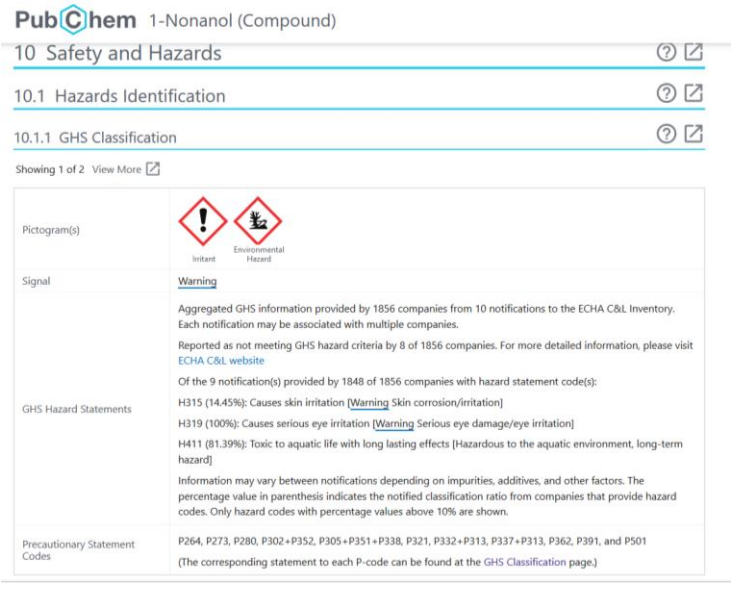

References

(1) Bruker-AXS. SAINT; Madison, Wisconsin, USA, 2017.
(2) Bruker-AXS. XPREP; Madison, Wisconsin, USA, 2017.
(3) Dolomanov, O.V., Bourhis, L.J., Gildea, R.J, Howard, J.A.K. & Puschmann, H. (2009), J. Appl. Cryst. 42, 339-341.
(4) Sheldrick, G.M. (2015). Acta Cryst. A71, 3-8.
(5) Sheldrick, G.M. (2015). Acta Cryst. C71, 3-8.
(6) Frisch, M. J.; Trucks, G. W.; Schlegel, H. B.; Scuseria, G. E.; Robb, M. A.; Cheeseman, J. R.; Scalmani, G.; Barone, V.; Petersson, G. A.; Nakatsuji, H.; Li, X.; Caricato, M.; Marenich, A. V.; Bloino, J.; Janesko, B. G.; Gomperts, R.; Mennucci, B.; Hratchian, H. P.; Ortiz, J. V.; Izmaylov, A. F.; Sonnenberg, J. L.; Williams-Young, D.; Ding, F.; Lipparini, F.; Egidi, F.; Goings, J.; Peng, B.; Petrone, A.; Henderson, T.; Ranasinghe, D.; Zakrzewski, V. G.; J. Gao; Rega, N.; Zheng, G.; Liang, W.; Hada, M.; Ehara, M.; Toyota, K.; Fukuda, R.; Hasegawa, J.; Ishida, M.; Nakajima, T.; Honda, Y.; Kitao, O.; Nakai, H.; Vreven, T.; Throssell, K.; J. A. Montgomery, J.; Peralta, J. E.; Ogliaro, F.; Bearpark, M. J.; Heyd, J. J.; Brothers, E. N.; Kudin, K. N.; Staroverov, V. N.; Keith, T. A.; Kobayashi, R.; Normand, J.; Raghavachari, K.; Rendell, A. P.; Burant, J. C.; Iyengar, S. S.; Tomasi, J.; Cossi, M.; Millam, J. M.; Klene, M.; Adamo, C.; Cammi, R.; Ochterski, J. W.; Martin, R. L.; Morokuma, K.; Farkas, O.; Foresman, J. B.; Fox, a. D. J. *Gaussian 16, Revision A.03*, Gaussian, Inc.: Wallingford CT, 2016.
(7) Zhao, Y.; Truhlar, D. G., The M06 suite of density functionals for main group thermochemistry, thermochemical kinetics, noncovalent interactions, excited states, and transition elements: two new functionals and systematic testing of four M06-class functionals and 12 other functionals. *Theoretical Chemistry Accounts* **2008,** *120* (1), 215-241.
(8) Hariharan, P. C.; Pople, J. A., The influence of polarization functions on molecular orbital hydrogenation energies. *Theoretical Chemistry Accounts* **1973,** *28* (3), 213-222.
(9) Petersson, G. A.; Bennett, A.; Tensfeldt, T. G.; AI-Laham, M. A.; Shirley, W. A.; Mantzaris, J., A complete basis set model chemistry. I. The total energies of closed-shell atoms and hydrides of the first-row elements *Journal of Chemical Physics* **1988,** *89* (4), 2193-2218.
(10) Petersson, G. A.; AI-Laham, M. A., A complete basis set model chemistry. II. Open-shell systems and the total energies of the first-row atoms *Journal of Chemical Physics* **1991,** *94* (9), 6081-6090.
(11) Marenich, A. V.; Cramer, C. J.; Truhlar, D. G., Universal Solvation Model Based on Solute Electron Density and on a Continuum Model of the Solvent Defined by the Bulk Dielectric Constant and Atomic Surface Tensions. *The Journal of Physical Chemistry B* **2009,** *113* (18), 6378-6396.
(12) Dennington, R.; Keith, T. A.; Millam, J. M. *GaussView, Version 5.0.9*, Semichem Inc., Shawnee Mission: KS, **2009**.
(13) Ho, J.; Zwicker, V. E.; Yuen, K. K. Y.; Jolliffe, K. A., Quantum Chemical Prediction of Equilibrium Acidities of Ureas, Deltamides, Squaramides, and Croconamides. *The Journal of Organic Chemistry* **2017,** *82* (19), 10732-10736.
(14) Shields, G. C.; Seybold, P. G., *Computational Approaches for the Prediction of pKa Values*. 1st Edition; CRC Press: Boca Raton, Florida, **2013**.

(15) Liptak, M. D.; Shields, G. C., Accurate pKa Calculations for Carboxylic Acids Using Complete Basis Set and Gaussian-n Models Combined with CPCM Continuum Solvation Methods. *Journal of the American Chemical Society* **2001,** *123* (30), 7314-7319.
(16) Chipman, D. M., Computation of pKa from Dielectric Continuum Theory. *The Journal of Physical Chemistry A* **2002,** *106* (32), 7413-7422.
(17) Ribeiro, R. F.; Marenich, A. V.; Cramer, C. J.; Truhlar, D. G., Use of Solution-Phase Vibrational Frequencies in Continuum Models for the Free Energy of Solvation. *The Journal of Physical Chemistry B* **2011,** *115* (49), 14556-14562.
(18) Ho, J., Are thermodynamic cycles necessary for continuum solvent calculation of pKas and reduction potentials? *Physical Chemistry Chemical Physics* **2015,** *17* (4), 2859-2868.
(19) Fifen, J. J.; Dhaouadi, Z.; Nsangou, M., Revision of the Thermodynamics of the Proton in Gas Phase. *The Journal of Physical Chemistry A* **2014,** *118* (46), 11090-11097.
(20) Lee, S.; Cho, K.-H.; Lee, C. J.; Kim, G. E.; Na, C. H.; In, Y.; No, K. T., Calculation of the Solvation Free Energy of Neutral and Ionic Molecules in Diverse Solvents. *Journal of Chemical Information and Modeling* **2011,** *51* (1), 105-114.
(21) Tehan, B. G.; Lloyd, E. J.; Wong, M. G.; Pitt, W. R.; Montana, J. G.; Manallack, D. T.; Gancia, E., Estimation of pKa Using Semiempirical Molecular Orbital Methods. Part 1: Application to Phenols and Carboxylic Acids. *Quantitative Structure-Activity Relationships* **2002,** *21* (5), 457-472.
(22) Tehan, B. G.; Lloyd, E. J.; Wong, M. G.; Pitt, W. R.; Gancia, E.; Manallack, D. T., Estimation of pKa Using Semiempirical Molecular Orbital Methods. Part 2: Application to Amines, Anilines and Various Nitrogen Containing Heterocyclic Compounds. *Quantitative Structure-Activity Relationships* **2002,** *21* (5), 473-485.